Available online at www.sciencedirect.com
SCIENCE DIRECT®
International Journal of Approximate Reasoning
41 (2006) 212–228
INTERNATIONAL JOURNAL OF APPROXIMATE REASONING
www.elsevier.com/locate/ijar

Rough fuzzy set based scale space transforms and their use in image analysis

A. Petrosino *, G. Salvi

Universitá di Napoli "Parthenope", Via A. De Gasperi 5, 80133 Napoli, Italy

Received 1 January 2004; received in revised form 1 May 2005; accepted 1 June 2005
Available online 16 September 2005

Abstract

In this paper we present a multi-scale method based on the hybrid notion of rough fuzzy sets, coming from the combination of two models of uncertainty like vagueness by handling rough sets and coarseness by handling fuzzy sets. Marrying both notions lead to consider, as instance, approximation of sets by means of similarity relations or fuzzy partitions. The most important features are extracted from the scale spaces by unsupervised cluster analysis, to successfully tackle image processing tasks. Here, we report some results achieved by applying the method to multi-class image segmentation and edge detection, but it can be shown to be successfully applied to texture discrimination problem too.

Keywords: Fuzzy rough sets; Clustering; Edge detection; Region segmentation

1. Introduction

Multi-scale representation is a very useful tool for handling image structures at different scales in a consistent manner. It was introduced in image analysis and computer vision by Marr, Witkin and others who appreciated that multi-scale analysis offers many benefits [3,8,11,15,25,26,33,35–38]. The basic idea is to embed the original signal $f: R^n \to R$ into a stack of signals filtered at increasing scales, in which the fine details are successively suppressed. The signal filtered at scale $\sigma \in R$ is a function $F: R^n \times R \to R$ defined by

* Corresponding author.
E-mail address: alfredo.petrosino@uniparthenope.it (A. Petrosino).

0888-613X/$ - see front matter
doi:10.1016/j.ijar.2005.06.015

$F(\mathbf{x};\sigma) = (O_\sigma(f))(\mathbf{x})$, where O_σ is a filter operator depending on σ, F is a function in an $(n+1)$-dimensional space, called scale space, and the collection of filtered signals is referred to as the multi-scale representation of f. The filter operation O_σ can be a linear operation (e.g. Gaussian smoothing) or a nonlinear operation (e.g. morphological filter).

Since the scale-space concept was introduced into image analysis and computer vision, its use has been firmly established, and there has been an emerging interest in incorporating scale-space operators as part of high-level computer vision tasks [21]. The output of the scale-space representation can be used for a variety of early visual tasks, from feature detection and feature classification to shape computation [25]. Several techniques for multi-scale morphological analysis exist, such as pyramids [8,18], size distributions, granulometries [7,27], morphological curvature scale space [24]. They are used to quantify the amount of detail in an image at different scales, with a consequent large variety of applications.

In this paper we propose to make scale space accordingly to the notion of rough fuzzy sets, realizing a system capable to efficiently cluster data coming from image analysis tasks. The hybrid notion of rough fuzzy sets comes from the combination of two models of uncertainty like vagueness by handling rough sets [28] and coarseness by handling fuzzy sets [39]. Rough sets embody the idea of indiscernibility between objects in a set, while fuzzy sets model the ill-definition of the boundary of a sub-class of this set. Marrying both notions lead to consider, as instance, approximation of sets by means of similarity relations or fuzzy partitions. The proposed multi-scale mechanism, based on the model of rough fuzzy sets, named C-calculus, introduced by Caianiello [9] is adopted to spread out local into more global information. The extracted features at different scales are clustered by minimizing the fuzziness of the output layer. This constitutes a fast algorithm for computing scale spaces, and applying them to image processing. We report results for (i) edge detection, (ii) region-based image segmentation, and (iii) texture segmentation.

The remainder of this paper is organized as follows. Section 2 briefly review the basic notions we shall adopt in the rest of paper. Section 3 presents the idea underlying our proposed approach and Section 4 reports how constructing scale spaces by adopting a fuzzy neural network. In Section 5 the effectiveness of the proposed model is shown when applied to some computer vision problems. Conclusions are drawn in Section 6.

2. Fuzzy sets, rough sets and *C*-sets

2.1. Rough sets

Let $X = \{x_1, \ldots, x_n\}$ be a set of U and R an equivalence relation on X. As usual, X/R denotes the quotient set of equivalence classes, which form a partition in X, i.e. xRy means the x and y cannot be took apart. The notion of *rough set* [28] borns to answer the question of how a subset T of a set X in U can be represented by means of X/R. It consists of two sets:

$$RS^*(T) = \{[x]_R | [x]_R \cap T \neq \emptyset\} \tag{1}$$

$$RS_*(T) = \{[x]_R | [x]_R \subseteq T\} \tag{2}$$

where $[x]_R$ denotes the class of elements $x, y \in X$ such that xRy. $RS^*(T)$ and $RS_*(T)$ are respectively the *upper* and *lower approximation* of T by R, i.e.

$$RS_*(T) \subseteq T \subseteq RS^*(T) \tag{3}$$

Other operations over rough sets include:

- Negative region of X: $U - RS^*(X)$.
- Boundary region of X: $RS^*(X) - RS_*(X)$.
- Quality of approximation of X by RS_* and RS^*: $\mu_R S(X) = \frac{\mathrm{card}(RS^*(X))}{\mathrm{card}(RS_*(X))}$.

2.2. Fuzzy sets

Fuzzy sets were introduced by Zadeh in 1965 [39] as a mean of representing and manipulating data that are not precise. Conventional (crisp) sets contain objects that satisfy precise properties required for membership: an object belongs or not to a set. Zadeh's theory provided a mechanism for measuring the degree to which an object belongs to a set by introducing the "membership degree" as a characteristic function $\mu_A(x)$ which associates with each point x a real number in the range $[0,1]$. The nearer the value of $\mu_A(x)$ to unity, the larger the membership degree of x in the set A.

Let us assume X be a set, then two different *crisp* versions of a fuzzy set A can be defined, namely $\bar{A} = \{(x, \mu_{\bar{A}}) | x \in X\}$ and $\underline{A} = \{(x, \mu_{\underline{A}}) \,|\, x \in X\}$ where

$$\mu_{\bar{A}}(x) = \begin{cases} 1 & \mu_A(x) \geqslant 0.5 \\ 0 & \mu_A(x) < 0.5 \end{cases} \tag{4}$$

and

$$\mu_{\underline{A}}(x) = \begin{cases} 1 & \mu_A(x) < 0.5 \\ 0 & \mu_A(x) \geqslant 0.5 \end{cases} \tag{5}$$

Moreover, denoting with $A \subset X$ and $B \subset X$ two fuzzy sets, i.e. $A = \{(x_i, \mu_A(x_i)), i = 1, \ldots, n\}$ and $B = \{(x_i, \mu_B(x_i)), i = 1, \ldots, n\}$, the operations on fuzzy sets are extensions of those used for conventional sets (intersection, union, comparison, etc.). The basic operations are the intersection and union as defined as follows:

The membership degree of the *intersection* $A \cap B$ is

$$\mu_{A \cap B}(x) = \min\{\mu_A(x), \mu_B(x)\} \quad x \in X \tag{6}$$

The membership degree of the *union* $A \cup B$ is

$$\mu_{A \cup B}(x) = \max\{\mu_A(x), \mu_B(x)\} \quad x \in X \tag{7}$$

Furthermore, a common measure of similarity between two fuzzy sets A and B is the l^p-distance, defined as follows.

The l^p-distance between two fuzzy sets A and B is given by

$$l^p(A, B) = \left(\sum_{i=1}^{n} |\mu_A(x_i) - \mu_B(x_i)|^p \right)^{1/p} \tag{8}$$

If $p = 1$ the l^p-distance reduces to the fuzzy Hamming distance.

The previous are only a restricted set of operations applicable among fuzzy sets, but they are the most significant for our aim. The definition of measures of fuzziness are also of interest for our aim.

Measures of fuzziness $F(A)$ of a fuzzy set $A = \{(x_i, \mu_A(x_i)),\ i = 1, \ldots, n\}$, n being the cardinality of A, give the average amount of ambiguity in making a decision whether an element belongs to the set or not. $F(A)$ has to be the following properties [19]:

(1) $F(A)$ is minimum when $\mu_A(x_i) = 0$ or $1\ \forall i$.
(2) $F(A)$ is maximum when $\mu_A(x_i) = 0.5\ \forall i$.
(3) $F(A) \geqslant F(B)$ iff

$$\mu_B(x_i) \geqslant \mu_A(x_i) \quad \text{if } \mu_A(x_i) \geqslant 0.5$$
$$\mu_B(x_i) \leqslant \mu_A(x_i) \quad \text{if } \mu_A(x_i) \leqslant 0.5$$

(4) $F(A) = F(\bar{A})$, $\bar{A}$ being the complement set of A, i.e. $\bar{A} = \{(x_i, 1 - \mu_A(x_i))\}$.

Along years, many authors have proposed different measures of fuzziness, i.e., *Kauffmann's Fuzziness* [20]

$$K_p(A) = \frac{2}{n^{1/p}} l^p(A, \bar{A}) \quad p \geqslant 1 \tag{9}$$

Specifically, if $p = 1$ the Kauffmann's Fuzziness is named Linear Index of Fuzziness (LIF) and assumes the following form:

$$\mathrm{LIF}(A) = \frac{2}{n} \sum_{i=1}^{n} \min\{\mu_A(x_i), (1 - \mu_A(x_i))\} \tag{10}$$

In addition, if $p = 2$ the Kauffmann's Fuzziness, named the Euclidean Index of Fuzziness (EIF), assumes the following form:

$$\mathrm{EIF}(A) = \frac{2}{\sqrt{n}} \sqrt{\sum_{i=1}^{n} \{\mu_A(x_i) - \mu_{A'}(x_i)\}^2} \tag{11}$$

Other measures of fuzziness include:

- *Kosko's Fuzziness* [22]

$$R_p(A) = \frac{l^p(A, \bar{A})}{l^p(A, \underline{A})} \quad p \geqslant 1 \tag{12}$$

- *De Luca, Termini's Fuzziness* [14]

$$E_k(A) = D_k(A) + D_k(A') \tag{13}$$

where $k > 0$ and $D_k(A) = -k \sum_i \mu_A(x_i) \log \mu_A(x_i)$.

2.3. C-sets

A *composite set* or *C-set* [9,2] is a triple $C = (\Gamma, m, M)$ where $\Gamma = \{X_1, \ldots, X_p\}$ is a partition of X in p disjoint subsets $X_1, \ldots, X_p$ and m, M are mappings of kind $X \to [0, 1]$ such that $\forall x \in X$, $m(x) = \sum m_i \mu_{X_i}(x)$ and $M(x) = \sum M_i \mu_{X_i}(x)$ where

$$m_i = \inf\{f(x) | x \in X_i\} \tag{14}$$
$$M_i = \sup\{f(x) | x \in X_i\} \tag{15}$$

for each choice of function $f: X \to [0,1]$. Γ and f uniquely define a composite set. If f is the membership function μ_F and the partition Γ is made with respect to a relation R, i.e. $\Gamma = X/R$, a fuzzy set F gets two approximations $RS^*(F)$ and $RS_*(F)$, which are again fuzzy sets with membership functions defined as (14) and (15), i.e. $m_i = \mu_{RS_*(F)}$ and $M_i = \mu_{RS^*(F)}$. The couple of sets $(RS^*(F), RS_*(F))$ is also called *rough fuzzy set* [16].

In addition to usual operations on fuzzy sets, like union and intersection, a basic operation is valid over these sets, called *C-product*. The operation *C*-product between couple of *C*-sets is defined as follows. Given two sets C and C', both related to different partitions of the same set X, the *C*-product, denoted as $\otimes$, is defined as the new *C*-set C'':

$$C'' = C \otimes C' = (\Gamma'', m'', M'') \tag{16}$$

where Γ'' is a new partition whose elements are

$$X''_{i,j} = X_i \cap X_j \tag{17}$$

and $m''_{i,j} = \max\{m_i, m'_j\}$, $M''_{i,j} = \min\{M_i, M'_j\}$. The *C*-product satisfies:

$$m(X) \leqslant m''(X) \leqslant \mu(X) \leqslant M''(X) \leqslant M(X) \tag{18}$$

and

$$m'(X) \leqslant m''(X) \leqslant \mu(X) \leqslant M''(X) \leqslant M'(X) \tag{19}$$

As shown in [16] this computation scheme generalizes the concept of fuzzy set to rough fuzzy set. It has been also demonstrated in [2,10] that recursive application of the previous operation provides a refinement of the original sets, realizing a powerful tool for measurement and a basic signal processing technique. Recently, it has been also shown that there is a tight relationship between rough sets and mathematical morphology [6], that gives evidence of the increasing interest of the image analysis researchers towards these theories.

3. The proposed multi-scale approach

Let us consider a set X of picture elements, i.e. a discretized Cartesian product $X = \{0,\ldots,N-1\} \times \{0,\ldots,M-1\}$. $[x]_R$ denotes the class of pixels containing x and μ is the luminance function of each pixel. A typical task in computer vision is to isolate subset of pixels which satisfy some specific criteria like chromatic or textural homogeneity (image segmentation), or are characterized by a local change in intensity (edge detection), etc. Given a subset T of the image not necessarily included or equal to any $[x]_R$, various approximations $RS^*(T)$ and $RS_*(T)$ of this subset may be obtained. This subset defines the contour or uniform regions in the image. On the contrary, regions appear rather like fuzzy sets of gray levels and their comparison or combination generates more or less uniform partitions of the image. It should be clear that rough sets and fuzzy sets are not rival theories but capture two distinct aspects of imperfection in knowledge, like indiscernibility and vagueness. Rough fuzzy sets, and in particular *C*-sets, seem to capture these aspects together, trying to extract different kinds of knowledge in data.

Local properties can be extracted by a multiresolution mechanism based on *C*-sets. In particular, let us consider four different partitions Γ^i, $i = 1,2,3,4$, of the set-image X, such that each element of Γ^i is a subimage of dimension $w \times w$ and Γ^2, Γ^3, Γ^4 are taken as shifted versions of Γ^1 in the directions of 0°, 90° and 45° of $w-1$ pixels. In such a case each pixel of the image can be seen as the intersection of four corresponding elements of the partitions Γ^1, Γ^2, Γ^3, Γ^4, as shown in Fig. 1. Since for each partition a *C*-set may

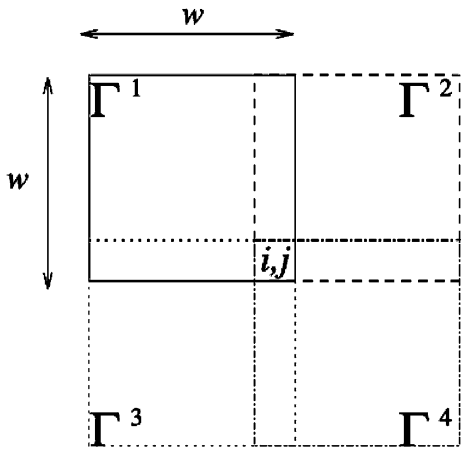

Fig. 1. Each image pixel can be seen as the intersection of four elements of the partitions Γ^1, Γ^2, Γ^3, Γ^4.

be defined, each pixel can be seen as belonging to the partition obtained by C-producting the original four C-sets:

$$\mathscr{C} = \mathscr{C}^1 \otimes \mathscr{C}^2 \otimes \mathscr{C}^3 \otimes \mathscr{C}^4 \tag{20}$$

where $\mathscr{C}^i$ is the composite set corresponding to partition Γ^i. In this case the *scale* is represented by the size w of each partition element.

In the sequel we shall refer to each $w \times w$ region as a candidate region to be categorized, i.e. *crc*. If the features extracted within a *crc* satisfy a specific constraint, e.g. homogeneity in the case of image segmentation, we shall refer to it as *rc* (region to be categorize) and take apart the features extracted.

The C-product operator is neither idempotent nor increasing. The fact that this operator is not idempotent allows it to be iteratively applied on the input signal in order to construct the scale space. Also, it is easy to see that the criterions in Eqs. (14) and (15) are not increasing, and therefore the operator is not increasing either.

It is also possible to formulate a filtering process by keeping the result of minima and maxima. The filtering results shown in Fig. 2 were obtained by applying (14) and (15) operators. That is, at each iteration k, the image I_k is filtered by a minimum operator over a window w producing m^w and by a maximum operator producing M^w. At the following iteration, the same operators are applied to both results m^w and M^w of the previous iteration.

Let us introduce the *multi-scale gradient* definition based on the previous operations.

Definition 1. Given the maxima and minima images (respectively M and m) generated by the application of the operation (20) over four different partitions of an image with a scale w, the *multi-scale gradient* at the position (i,j) is

$$G^w_{i,j} = M^w_{i,j} - m^w_{i,j} \tag{21}$$

This operation corresponds to the difference between the lower and upper approximation of a fuzzy set. To extract gradient information at different scales, the gradient operation (21) should be applied by using increasing values of w and generating a multichannel image (Fig. 3).

Fig. 2. Scale space filtering by C-producting four C-sets with $w = 3$, $w = 5$ and $w = 9$. First row: m^3, m^5, m^9; second row: M^3, M^5, M^9.

Fig. 3. Multi-scale gradient filtering with $w = 3$, $w = 5$, $w = 9$. By column: G^3, G^5, G^9.

An important advantage of the scale space transform over linear diffusion, as filtering tools, or gradient filtering is that they do not introduce new contours, i.e. it is edge preserving. Although nonlinear anisotropic diffusion overcomes this problem, the choice of the diffusivity function is not always obvious. Contrary to anisotropic diffusion, the proposed scale space transform is parameter-free. Other advantages of using this representation for image analysis tasks are discussed in the next sections.

4. Constructing *n*-dimensional scale spaces

The multi-scale construction may follow that of a fuzzy neural network [23,34]. Specifically, it consists into two pyramidal-layered networks with fixed weights, each looking upon an $2^n \times 2^n$ image. By fixing the initial dimension $w = 2^L$ of *crc*, each pyramidal

network is constituted by $n - L$ multiresolution levels. Each processing element (i,j) at the lth level of the first pyramid (second pyramid) computes the minimum value (maximum value) over a $2w \times 2w$ area at the $(l-1)$th level. The pyramidal structures are computed in a top–down manner, firstly analyzing regions as large as possible and then proceeding by splitting regions turned out to be not of interest. The mechanism of splitting is the following.

If we suppose to be at the lth level of both pyramid-networks and analyze a region $w \times w$ which is the intersection of four $2w \times 2w$ regions, the minimum and maximum values computed inside are denoted by $m_{k,l}$ and $M_{k,l}$, $k = i, \ldots, i+w$, $l = j, \ldots, j+w$. The combination of the minima and maxima values is made up at the output layer, i.e.

$$a^1_{i,j} = \min_{k\in\{i,\ldots,i+w\}l\in\{j,\ldots,j+w\}} M_{k,l} \quad a^2_{i,j} = \max_{k\in\{i,\ldots,i+w\}l\in\{j,\ldots,j+w\}} m_{k,l} \tag{22}$$

If $a^1_{i,j}$ and $a^2_{i,j}$ satisfy a specific constraint, the region under consideration is seen as *rc* and the values are retained as elementary features of such a region. Otherwise, the region is divided in four sub-regions with dimension equal to $w/2$. The preprocessing sub-network is applied again to the newly defined regions. The process is continued until the convergence criterion is satisfied and no more regions of dimension greater than 2 remains. The extracted features are representative of all regions under the specific constraint.

Each *crc* belongs to different partitions of the input image, while each partition element is a set of neighboring pixels of the *crc*, characterized only by two intensity levels inside the set itself: the lowest and the highest intensities. These values measure the degree of being nearer to the background or, respectively, to the foreground. In particular, for edge detection, the classification of each *crc* must be aimed at the identification of the abrupt changes of the gray-level pattern on the neighborhood of each *crc*. To this purpose, the fuzzy intersections computed by the preprocessing subnetwork are fed to a classification subnetwork which is described in the following.

4.1. Clustering subnetwork

Each node in the clustering subnetwork receives, as shown in Fig. 4, two input values from each corresponding neuron at the previous layer. In particular, at each iteration, a learning step is applied to the clustering subnetwork according to the minimization of a *Fuzzines Index* (FI), applying, and somewhere extending, the learning mechanism proposed in [17]. The output of a node j is then obtained as

$$\begin{aligned} o_j &= f(I_j) \\ I_j &= g(\underline{O}_i, \underline{W}_{ji}) \end{aligned} \tag{23}$$

where $\underline{O}_i = (o^{2,1}_i, o^{2,2}_i)$ and $\underline{W}_{ji} = (w^1_{j,i}, w^2_{j,i})$ where $w^q_{j,i}$ indicates the connection weight between the jth node of the output layer and the ith node of the previous layer in the qth cell-plane, $q = 1,2$. Each sum is intended over all nodes i in the neighborhood of the jth node at the upper hidden layer. f (the *membership function*) can be sigmoidal, hyperbolic, Gaussian, Gaborian, etc. with the accordance that if o_j takes the value 0.5, a small quantity (usually 0.001) is added; this reflects into dropping out unstability conditions. g is a similarity function, e.g. correlation, Minkowsky distance, etc.

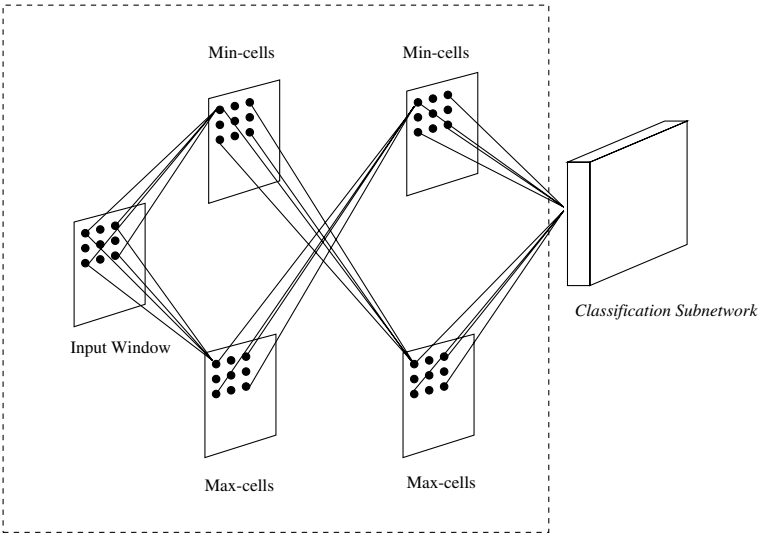

Fig. 4. The preprocessing networks is based on a set of fixed weight modules each performing a C-intersection between four sets of data each consisting of a $2w \times 2w$ window of the input image. The output of the network is then fed to a classification stage aimed at categorization its inputs into classes of interest.

To retain the value of each output node o_j in $[0,1]$, we apply the following mapping to each input image pixel g

$$g' = \frac{g - g_{\min}}{g_{\max} - g_{\min}} \tag{24}$$

where $g_{\min}$ and $g_{\max}$ are the lowest and highest gray levels in the image.

4.2. Learning

The subnetwork has to self-organize by minimizing the fuzziness of the output layer. This is an iterative process with a feedback mechanism which provides the input layer with new pixel values (the neuron activities of the output layer), so continuing the "learning" until convergence. Since the membership function is chosen to be sigmoidal, minimizing the fuzziness is equivalent to minimizing the distances between corresponding pixel values in both cell-planes at the upper hidden layer. To this aim the weights $w^1_{j,i}$ and $w^2_{j,i}$ are set respectively as excitatory and inhibitory. Since random initialization acts as noise, *all the weights are initially set to unity*. The adjustment of weights is done using the gradient descent search, i.e. the incremental change $\Delta w^l_{j,i}$, $l = 1,2$, is taken as proportional to the sum of the negative gradient $-\eta \frac{\partial E}{\partial o_i} f'(I_i) o_j$. The adjustment rule is then the following:

$$w^l_{j,i} = w^l_{j,i} + \eta \Delta w^l_{j,i} \tag{25}$$

Specifically, we adopted the Linear Index of Fuzziness and the Euclidean Index of Fuzziness, whose updating rules look as follows, where E indicates the energy-fuzziness of our system and $n = M \times N$.

- Linear Index of Fuzziness (LIF) learning:

$$\Delta w^1_{j,i} = \begin{cases} -\eta_{\mathrm{LIF}}(1-o_j)o_j o_i^{2,2} & \text{if } 0 \leqslant o_j \leqslant 0.5 \\ \eta_{\mathrm{LIF}}(1-o_j)o_j o_i^{2,2} & \text{if } 0.5 < o_j \leqslant 1 \end{cases} \tag{26}$$

$$\Delta w^2_{j,i} = \begin{cases} -\eta_{\mathrm{LIF}}(1-o_j)o_j o_i^{2,1} & \text{if } 0 \leqslant o_j \leqslant 0.5 \\ \eta_{\mathrm{LIF}}(1-o_j)o_j o_i^{2,1} & \text{if } 0.5 < o_j \leqslant 1 \end{cases} \tag{27}$$

where $\eta_{\mathrm{LIF}} = \eta \times 2/n$.

- Euclidean Index of Fuzziness (EIF) learning:

$$\Delta w^1_{j,i} = \begin{cases} -\eta_{\mathrm{EIF}}(1-o_j)o_j^2 o_i^{2,2} & \text{if } 0 \leqslant o_j \leqslant 0.5 \\ \eta_{\mathrm{EIF}}(1-o_j)^2 o_j o_i^{2,2} & \text{if } 0.5 < o_j \leqslant 1 \end{cases} \tag{28}$$

$$\Delta w^2_{j,i} = \begin{cases} -\eta_{\mathrm{EIF}}(1-o_j)o_j^2 o_i^{2,1} & \text{if } 0 \leqslant o_j \leqslant 0.5 \\ \eta_{\mathrm{EIF}}(1-o_j)^2 o_j o_i^{2,1} & \text{if } 0.5 < o_j \leqslant 1 \end{cases} \tag{29}$$

where $\eta_{\mathrm{EIF}} = \eta \times 2/\sqrt{(n)}$.

The previous rules hold also for the determination of an exact threshold value, θ, adopted for binarizing the image, e.g. in edge detection, when convergence is reached.

According to the properties of fuzziness the initial threshold is set to be 0.5; this value allows to determine an hard decision from an unstable condition to a stable one.

As said before, the updating of weights is continued until the network stabilizes. The system is said *stable* (the learning stops) when

$$E(t+1) \leqslant E(t) \quad \text{and} \quad |O(t+1) - O(t)| \leqslant \gamma \tag{30}$$

where $E(t)$ is the system fuzziness computed at the tth iteration, γ is a prefixed very small positive quantity and $O(t) = \sum_{j:o_j>=0.5} o_j$. After convergence, the pixels j satisfying some criterion are taken apart. As instance, for edge detection, the pixels j with $o_j > \theta$ are considered to constitute the edge map of the image; they are set to take value 1, in contrast with the remaining which will constitute the background (value 0).

5. Experimental results

In this section we describe the data sets used for experiments, the preprocessing steps of the input signals, the construction of the pattern vectors, and report classification results.

5.1. Edge detection

During experiments, we focus our attention on two aspects: (i) the ability of the system to detect true edges and neglect spurious edges; (ii) the robustness of the system when applied to noise corrupted versions of the images; (iii) the convergence time of the system with a prefixed value of γ.

Edge points can be thought of as pixel locations of abrupt gray-level or texture changes; such points of discontinuity could indicate the end of a region and the beginning of another. Detecting discontinuities within discrete signals such as images is based on numerical differentiation which is ill-posed [4], due to the noise amplification in computing derivatives. To overcome such problem it is common use to perform a smoothing (e.g.

convolution with a Gaussian mask) before computing the derivative. However, smoothing and accurate edge localization are contrasting concepts and constitute the main low-level vision dilemma. Here we will show how the theory of rough fuzzy set can be efficiently applied to tackle the problem of edge detection in gray-level images. In particular, our edge detection method does not include any smoothing step as it is based on rough fuzzy gradient operator which, as we will show, produce a smooth gradient map through the use of the proposed scale-space transform.

In each experiment, we applied the neural system described in the previous section adopting a neighborhood size of a neuron in the first and second layers equal to $w = 2$. In this case we analyze the local properties within a 3×3 region around each neuron. On the contrary, a neuron in the output layer looks at exactly two neurons, each belonging to a cell-plane at the upper hidden layer. The learning rate η_{LIF} has been taken as 0.2 while the convergence parameter γ has been taken to be 0.001. The reason for these choices resides in a most successful edge detection system, both for detecting edges and for suppressing noise, while requiring the minimum amount of computation or, equivalently, the minimum number of iterations to converge.

The upper-left image in Fig. 5 shows the image of size 512×480 and 174 gray levels (the face of *Lenna*), that contains several types of edges such as continuous and step edges. The proposed system has been used to detect edges in the case of noise corruption. The noisy versions were obtained by adding noise from a Gaussian $N(0, \sigma^2)$ distribution with different values of the standard deviation σ corresponding to the 3%, 6% and 12% of the dynamic range. The same Fig. 5 shows the edge images obtained applying the system to both images with the fuzziness calculated by using the Linear Index of Fuzziness. The same results are obtained by the Euclidean Index of Fuzziness. Since the learning rate of the EIF is low compared with the LIF, the number of iterations is the same; only the parameter η_{EIF} for the EIF is selected to be greater than the LIF one (η_{LIF}). In all the experiments made, and not only those reported, the system converged after six iterations, using a parameter value $\eta_{\mathrm{EIF}} = 2 \times \eta_{\mathrm{LIF}}$. For a fixed η value, the system converges in approximately the same number of iterations for any image we provide as input. Furthermore, the values of the threshold θ were automatically found by using the updating rules (26)–(29); they are all around the value 0.5 which corresponds to the total unstability condition for output neurons.

Examining the results, as the noise increases, the quality of the edge image, as expected, deteriorates, but true edges are mostly saved. The main advantages of the system comes from the fully automatic procedure to choice the exact threshold θ and from operating directly on the luminance images. This allows to detect fine edges, suppressing false edges usually present in real images. Other advantages are the fixed analysis window size at any level of the neural network structure and the computational load quite fixed also in presence of noise.

5.2. Multi-class image segmentation

To realize a multi-class image segmentation, a *crc* must satisfy an homogeneity constraint, i.e. the difference between $a^1_{i,j}$ and $a^2_{i,j}$ must be less or equal to a prefixed threshold θ. In such a case the region is seen as uniform and becomes *rc*, otherwise the *crc* is splitted into four newly defined *crc*'s, letting w be $w/2$. Several experiments were performed on real images to test the efficacy of the proposed method compared with the split and merge algo-

Fig. 5. In each row the original image corrupted by white noise ($\sigma = 3\%, 6\%, 12\%$ of the dynamic range) and the edge map obtained by the local operator Kirsh, Prewitt, Sobel and our method.

rithm [31] and the Fuzzy C-Means (FCM) algorithm [5], also adopted for similar aims in [32]. Here, we report the results achieved by applying these algorithms to a magnetic resonance image of a brain affected by tumor. Other results can be found in [30].

The parameters in our experiments have been set to the following values:

- $w_0 = 16$, $w_t = w_{t-1}/2$ (t means iteration);
- $\theta = 40$;

- $\eta = 0.1$ (learning rate);
- $\gamma = 0.001$ (convergence rate).

The maximum number of regions for segmenting the image has been set to 10, but only five classes have been generated by the clustering network after six iterations of the weight adjustment. In order to make comparisons, in split and merge and FCM algorithms the number of classes used for segmentation has been fixed to 5 and they reached convergence after twenty and fifteen iterations respectively. As shown, the proposed method produced a segmented image with better defined boundaries. Specifically, due to acquisition noise the parenchyma is not detected at all by the FCM, while is too confused in the segmentation result produced by the split and merge algorithm (Figs. 6(b) and 6(c)) (see also Fig. 7).

5.3. Texture separation

Here we adopt a multi-scale representation of the image resulting from a continuous morphological filtering modeled by a diffusion equation. Specifically, the adopted diffusion process is governed by the *Affine Morphological Scale Space* (AMSS) model introduced in [1] and defined as the solution of the following second order nonlinear partial differential equation:

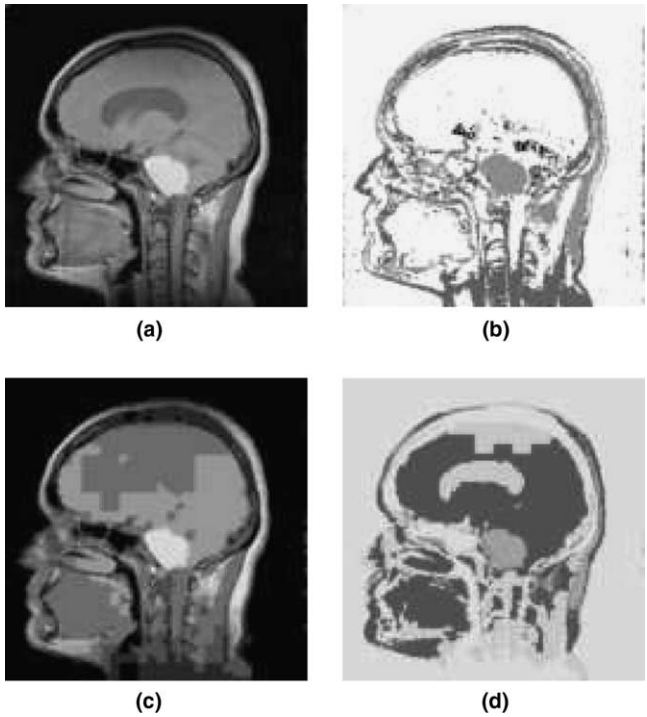

Fig. 6. Segmented versions of (a), obtained by applying the FCM (b), the split and merge algorithm (c) and the proposed method (d).

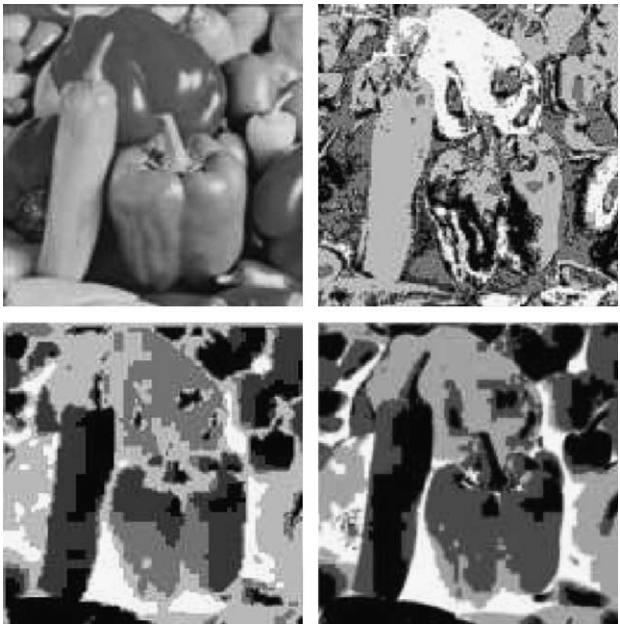

Fig. 7. In row order the original image, the segmented result of the histogram clustering by the FCM algorithm, the applied to the until convergence.

$$\frac{\partial u}{\partial t} = |\nabla u|(\mathrm{curv}(u))^{\frac{1}{3}} \quad u(\mathbf{x},0) = u_0(\mathbf{x}) \tag{31}$$

where curv(u) represents a second order differential operator corresponding to the curvature of level curves of $u(\mathbf{x},t)$, *i.e.* $\mathrm{curv}(u) = \frac{u_{xx}u_y^2 - 2u_{xy}u_x u_y + u_{yy}u_x^2}{(u_x^2+u_y^2)^{3/2}}$. Here the notation u_x represents the partial derivative of u with respect to the variable x and analogously for the other differential operators. Such equation has the property of moving the level sets of the image with a speed proportional to the curvature of such curves. The iterative application of the model (31) generates a multichannel image which encode information concerning about how the level sets regularize by model (31).

The *detail images*, as defined in Eq. (32), provide information about how the level curves move during the evolution of Eq. (31) representing the structure of the textural patterns in terms of difference between the level curves at different ''times''. The detail images are obtained as differences between the images analyzed at successive scales

$$d_i(\mathbf{x}) = u(\mathbf{x},t_i) - u(\mathbf{x},t_{i-1}) \tag{32}$$

with the scale parameter t discretized as a sequence of increasing values $t_0 = 0, t_1, t_2, \ldots, t_n$.

On the boundary between two textures the evolution ceases to be uniform and the fuzzy gradient operation is aimed at the detection of discontinuities in the sequence of detail images. Boundary localization is then performed by clustering a set of fuzzy gradient images extracted by the multi-scale representation of the input image. Here, instead of using a Fuzziness Index, the variational region growing algorithm, reported in [29], turned out to be more advantageous, producing the result depicted in of Fig. 8(b) where the two

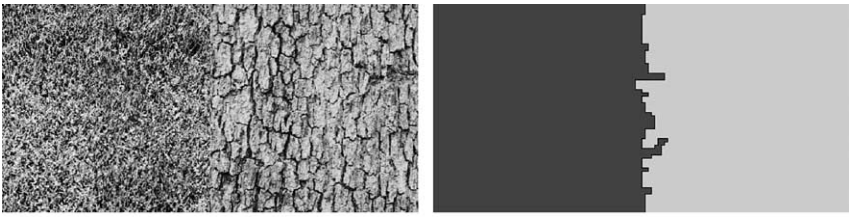

Fig. 8. An original textured image (a) and the result of the texture separation process (b).

textures depicted in Fig. 8(a) are efficiently separated. For a complete treatment of this application and a quantitative assessment of the algorithm, see [12]. The same approach for discriminate textures has been recently applied to retrieve by content textured images from an image database. See for details [13].

6. Conclusions

The paper reports a method for facing image analysis tasks based on rough fuzzy set scale space transforms, combined with unsupervised cluster analysis, which can be used for edge detection, region-based segmentation and texture separation. The advantages of using the proposed scale-space transform reside in capturing a reduced number of scale space entries, all characterizing different (fuzzy) aspects of the same object in the image.

The integration of the rough fuzzy set based scale space transform and neural clustering is also proposed for the realization of a specialized network. The integration is made by a hierarchical approach, subdividing the network in two sub-networks. The preprocessing sub-network is specialized to detect the relevant features inside each meaningful region by a multiresolution fuzzy method, while the second sub-network self-organizes to cluster in a fuzzy manner the features in a restricted number of classes.

The capability to extract well-defined and descriptive regions, also in real images, while the computational capability does not increase, makes valid the proposed approach and puts the basis for more insights in the study of such a system.

References

[1] L. Alvarez, F. Guichard, P.L. Lions, J.M. Morel, Axioms and fundamental equations of image processing, Archives for Rational Mechanics and Analysis 123 (3) (1993) 199–257.
[2] A. Apostolico, E.R. Caianiello, E. Fischetti, S. Vitulano, *C*-Calculus: an elementary approach to some problems in pattern recognition, Pattern Recognition 19 (1878) 375–387.
[3] J.A. Bangham, P.D. Ling, R. Harvey, Scale-space from nonlinear filters, IEEE Transactions on Pattern Analysis and Machine Intelligence 18 (1996) 520–528.
[4] M. Bertero, T.A. Poggio, V. Torre, Ill-posed problems in early vision, Proceedings of the IEEE 76 (1988) 869–889.
[5] J.C. Bezdek, Pattern Recognition with Fuzzy Objective Function Algorithms, Plenum Press, New York, 1981.
[6] I. Bloch, On links on between mathematical morphology and rough sets, Pattern Recognition 33 (9) (2000) 1487–1496.

[7] E.J. Breen, R. Jones, Attribute openings, thinnings and granulometries, Computer Vision Image Understanding 64 (3) (1996) 377–389.
[8] P.S. Burt, Attention mechanism for vision in a dynamic world, in: Proceedings of the 11th International Conference on Pattern Recognition, 1988, pp. 977–987.
[9] E.R. Caianiello, A calculus of hierarchical systems, in: Proceedings of the International Conference on Pattern Recognition, Washington DC, 1973.
[10] E.R. Caianiello, A. Petrosino, Neural Networks, fuzziness, image processing, in: V. Cantoni (Ed.), Machine and Human Perception: Analogies and Divergencies, Plenum Press, New York, 1994, pp. 355–370.
[11] V. Cantoni, L. Cinque, C. Guerra, S. Levialdi, L. Lombardi, 2-D object recognition by multiscale tree matching, Pattern Recognition 31 (10) (1998) 1443–1454.
[12] M. Ceccarelli, A. Petrosino, A parallel fuzzy scale-space approach to the unsupervised texture separation, Pattern Recognition Letters 23 (2002) 557–567.
[13] M. Ceccarelli, F. Musacchia, A. Petrosino, in: M. Frucci et al. (Eds.), A Fuzzy Scale-Space Approach to Feature-based Image Representation and Retrieval, Lecture Notes in Computer Science—BV&AI2005, Springer Verlag, 2005.
[14] A. De Luca, S. Termini, A definition of nonprobabilistic entropy in the setting of fuzzy sets theory, Information and Control 20 (1972) 301–312.
[15] C.R. Dyer, Multiscale image understanding, in: L. Uhr (Ed.), Parallel Computer Vision, Academic Press, New York, 1987, pp. 171–213.
[16] D. Dubois, H. Prade, Rough fuzzy sets and fuzzy rough sets, International Journal of General Systems 17 (1990) 119–209.
[17] A. Ghosh, N.R. Pal, S.K. Pal, Self-organization for object extraction and multilayer neural network and fuzziness measures, IEEE Transactions on Fuzzy Systems 1 (1993) 54–68.
[18] J. Goutsias, H.J.A.M. Heijmans, Multiresolution signal decomposition schemes, Part 1: Linear and morphological pyramids, IEEE Transactions on Image Processing 9 (11) (2000) 1862–1876.
[19] A. Kandel, Fuzzy Mathematical Techniques with Applications, New York, Addison-Wesley, 1986.
[20] A. Kauffmann, Introduction to the Theory of Fuzzy Subsets, vol. 1, Academic Press, New York, p. 197.
[21] T. Koller, G.S.G. Grieg, D. Dettwiler, Multiscale detection of curvilinear structures in 2D and 3D image data, in: Fifth International Conference on Computer Vision, Cambridge, MA, 1995, pp. 864–869.
[22] B. Kosko, Fuzziness vs. probability, International Journal of General Systems 17 (1990) 211–240.
[23] S. Lee, E. Lee, Fuzzy neural networks, Mathematical Biosciences 23 (1975) 151–177.
[24] F. Leymarie, M.D. Levine, Curvature morphology, Technical report TR-CIM-88-26, Computer Vision and Robotics Laboratory, McGill University, Montreal, Canada, 1988.
[25] T. Lindeberg, Scale-space theory: a basic tool for analysing structures at different scales, Journal of Applied Statistics 21 (1994) 225–270.
[26] D. Marr, S. Ullman, T. Poggio, Bandpass channels, zero-crossing, and early visual information processing, Journal of the Optical Society of America 69 (1979) 914–916.
[27] P.F.M. Nacken, Chamfer metrics, the medial axis and mathematical morphology, Journal of Mathematical Imaging and Vision 6 (1996) 235–248.
[28] Z. Pawlak, Rough sets, International Journal of Information and Computer Science 11 (5) (1982) 341–356.
[29] A. Petrosino, M. Ceccarelli, A scale-space approach to unsupervised texture separation, in: Proceedings of ICIAP'99, IEEE Press, 1999, pp. 162–169.
[30] A. Petrosino, M. Marsella, in: M. Marinaro, R. Tagliaferri (Eds.), Neural Fuzzy Segmentation by a Hierarchical Approach, Neural Nets WIRN'95, World Scientific Pub., Singapore, 1995.
[31] M. Pietikainen, A. Rosenfeld, Split and merge link algorithm for image segmentation, Pattern Recognition 15 (1982).
[32] M.R. Rezaee, P.M.J. van der Zwet, B.P.F. Lelieveldt, R.J. van der Geest, J.H.C. Reiber, A multiresolution image segmentation technique based on pyramidal segmentation and fuzzy clustering, IEEE Transactions on Image Processing 9 (7) (2000) 1238–1248.
[33] A. Rosenfeld (Ed.), Multiresolution Image Processing and Analysis, Springer, Berlin, 1984.
[34] P.K. Simpson, Fuzzy min–max neural networks—Part I: Classification, IEEE Transactions on Neural Networks 3 (1992) 776–786.
[35] N. Ueda, S. Suzuki, Learning visual models from shape contours using multi-scale convex/concave structure matching, IEEE Transactions on Pattern Analysis and Machine Intelligence 15 (4) (1993) 337–352.
[36] P.T. Jackway, M. Deriche, Scale-space properties of the multiscale morphological dilation–erosion, IEEE Transactions on Pattern Analysis and Machine Intelligence 18 (1996) 38–51.

[37] A.C. Jalba, M.H.F. Wilkinson, J.B.T.M. Roerdink, Morphological hat-transform scale spaces and their use in pattern classification, Pattern Recognition 37 (2004) 901–915.
[38] A.P. Witkin, Scale-space filtering, in: Proceedings of the International Joint Conference on Artificial Intelligence, Palo Alto, CA, pp. 1019–1022, 1983.
[39] L.A. Zadeh, Fuzzy sets, Information and Control 8 (1965) 338–353.